Generation and Evolution of a Cyclonic Ring at Drake Passage in Early 1979

R. G. PETERSON, W. D. NOWLIN, JR., AND T. WHITWORTH III

Department of Oceanography, Texas A&M University, College Station 77843

(Manuscript received 11 December 1981, in final form 22 March 1982)

ABSTRACT

An equatorward meander in the Antarctic Polar Front at Drake Passage was observed to amplify and pinch off during January and early February 1979, forming a cold-core cyclonic current ring with a radius of ~50 km. This ring appeared to move directly across the Passage parallel to a submarine ridge before turning northeastward upon reaching a gap between the ridge and the South American continental rise. Its net motion was across the Polar Frontal Zone and the ring was last observed to be pushing through the Subantarctic Front. Geostrophic surface speeds of up to 90 cm s^{-1} relative to 3500 m were observed where the northern sector of the ring and the Subantarctic Front were in proximity. A stability analysis of the banded flow regime across Drake Passage suggests that necessary conditions for baroclinic instability exist everywhere within the zonal current and those for barotropic instability exist adjacent to the fronts. The heat and salt anomalies of this ring relative to the Polar Frontal Zone are estimated as -8×10^{18} J and -2×10^{11} kg, respectively, and relative to the Subantarctic Zone as -3×10^{19} J and -8×10^{11} kg, respectively. The process of ring migration across these fronts is potentially important to the heat and salt budgets of the Southern Ocean.

1. Introduction

The Antarctic Convergence, or Polar Front, was first observed by Meinardus (1923) as a large meridional surface temperature gradient separating the Antarctic and Subantarctic waters, and was later shown by Deacon (1937) to be a continuous feature in the Southern Ocean. Mackintosh (1946) observed pronounced latitudinal variations in the position of this front, along with isolated rings shed from the meanders, and speculated that the boundary is an unstable one. The Polar Front is now known to be accompanied by additional fronts. Four distinct zones, each possessing individual temperature-salinity characteristics have been identified south of Australia (Gordon *et al.*, 1974), in the western Scotia Sea east of Drake Passage (Gordon *et al.*, 1977) and in Drake Passage (Nowlin *et al.*, 1977). The four zones are separated by fronts which are characterized by large horizontal density gradients and high geostrophic speeds.

From north to south, the four zones and three fronts are (after Whitworth, 1980): Subantarctic Zone (SAZ), Subantarctic Front (SAF), Polar Frontal Zone (PFZ), Polar Front (PF), Antarctic Zone (AZ), Continental Water Boundary (CWB) and Continental Zone (CZ). Fig. 1 shows the locations of these zones and fronts as they existed in Drake Passage during late February 1976. The vertically-averaged geostrophic speeds relative to 2500 m along this transect show the through-Passage components of flow as might be typically observed.

Recent investigations have shown that the necessary conditions for instability as specified by a simple linear baroclinic-instability model are satisfied by a uniform flow field across Drake Passage (Bryden, 1979; Wright, 1981). Accordingly, the available potential energy (APE) associated with tilted isopycnals may be released to perturbations imposed on the basic state, resulting in wave growth and possible ring formation. The process of wave growth and ring formation has been observed in Drake Passage (Joyce and Patterson, 1977), south of Australia (Savchenko *et al.*, 1978) and elsewhere. Bryden (1981) summarized the observations of rings within the Antarctic Circumpolar Current (ACC), stating that they vary in radius from 30 km in Drake Passage to 100 km elsewhere and have surface velocities of 30 cm s^{-1} or greater.

One of the objectives of the Dynamic Response and Kinematics Experiment of 1979 (DRAKE 79), a part of the International Southern Ocean Studies (ISOS) program, was to describe mesoscale features occurring within the ACC system. This study describes the formation and migration of a cold-core cyclonic ring in Drake Passage and some effects it had on the ACC structure. The heat and salt anomalies associated with the ring are calculated relative to PFZ and SAZ waters and compared with estimates made by Joyce *et al.* (1981). The hydrodynamic stability of a basic ACC flow regime with zonation and the possible effects of topography on the ring are investigated.

0022-3670/82/070712-08$06.00
© 1982 American Meteorological Society

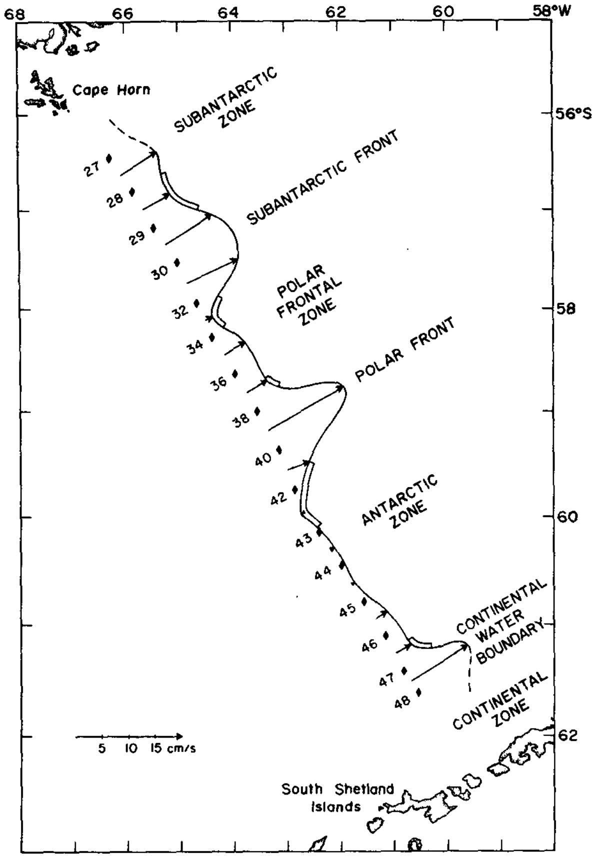

FIG. 1. Vertically-averaged geostrophic speeds relative to 2500 m in direction normal to station pairs occupied from R/V *Thompson* during 28 Feb–3 Mar 1976. Double contours demark regions where $\beta - U_{yy} < 0$.

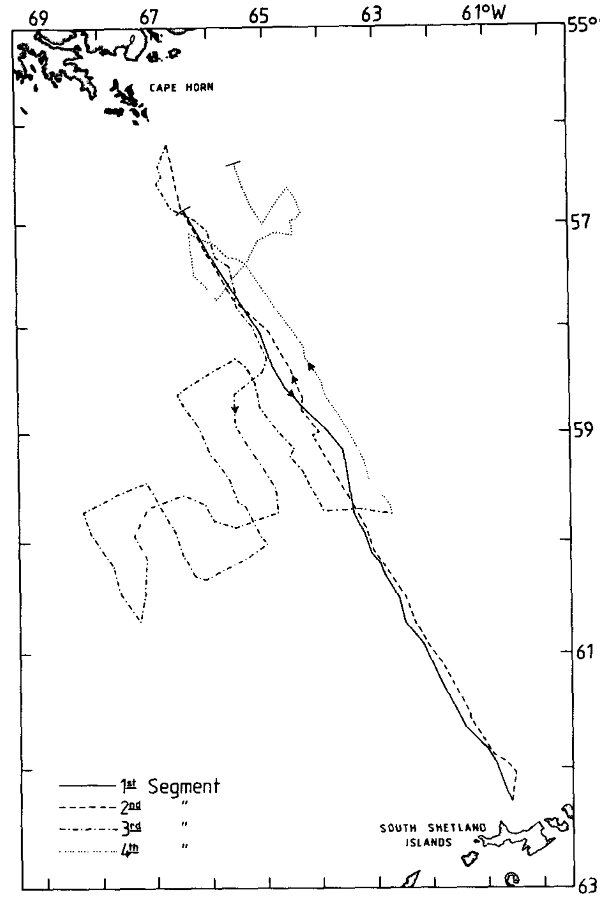

FIG. 2. Cruise track of R/V *Melville* during DRAKE 79: segment 1, 14–18 Jan; segment 2, 23–24 Jan; segment 3, 25 Jan–3 Feb; segment 4, 3–5 Feb.

2. Data and observations

As part of DRAKE 79, the R/V *Melville* made a cruise within Drake Passage during January and early February 1979, during which a moored array was deployed, hydrographic stations were occupied and XBT data were collected. Two complete transects of the Passage were followed by a more detailed survey of the central and northern portions of the Passage. For our analysis, we have divided the cruise into four segments (Fig. 2) and treated each as being synoptic.

Vertical temperature cross-sections to 500-m depth for each cruise segment showed cold AZ water intruding progressively farther into the warmer PFZ. The early meridional displacement of the intrusion away from the AZ is seen in the first two segments (Fig. 3). The temperature minimum within the AZ deepened from ~80 m north of the Antarctic continental shelf to about 125 m near the PF, with vertical variations of up to 30 m. The coldest water within the T-minimum layer was found in pockets which advected with the flow. During the first cruise segment, the T-minimum of the intrusion was found near 150 m depth. In subsequent sections, as the ring moved northward, this layer continued to deepen. By the end of the study period it was centered near 225 m and the 2°C isotherm that enclosed the T-minimum layer had extended to deeper than 500 m.

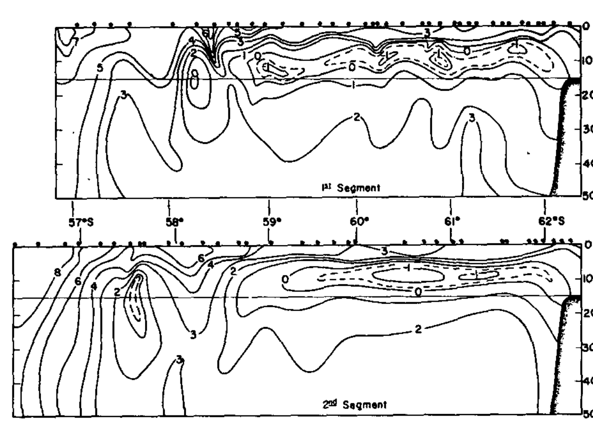

FIG. 3. Temperature fields across Drake Passage as constructed from XBT data taken during *Melville* cruise segments 1 and 2. Dots indicate XBT positions.

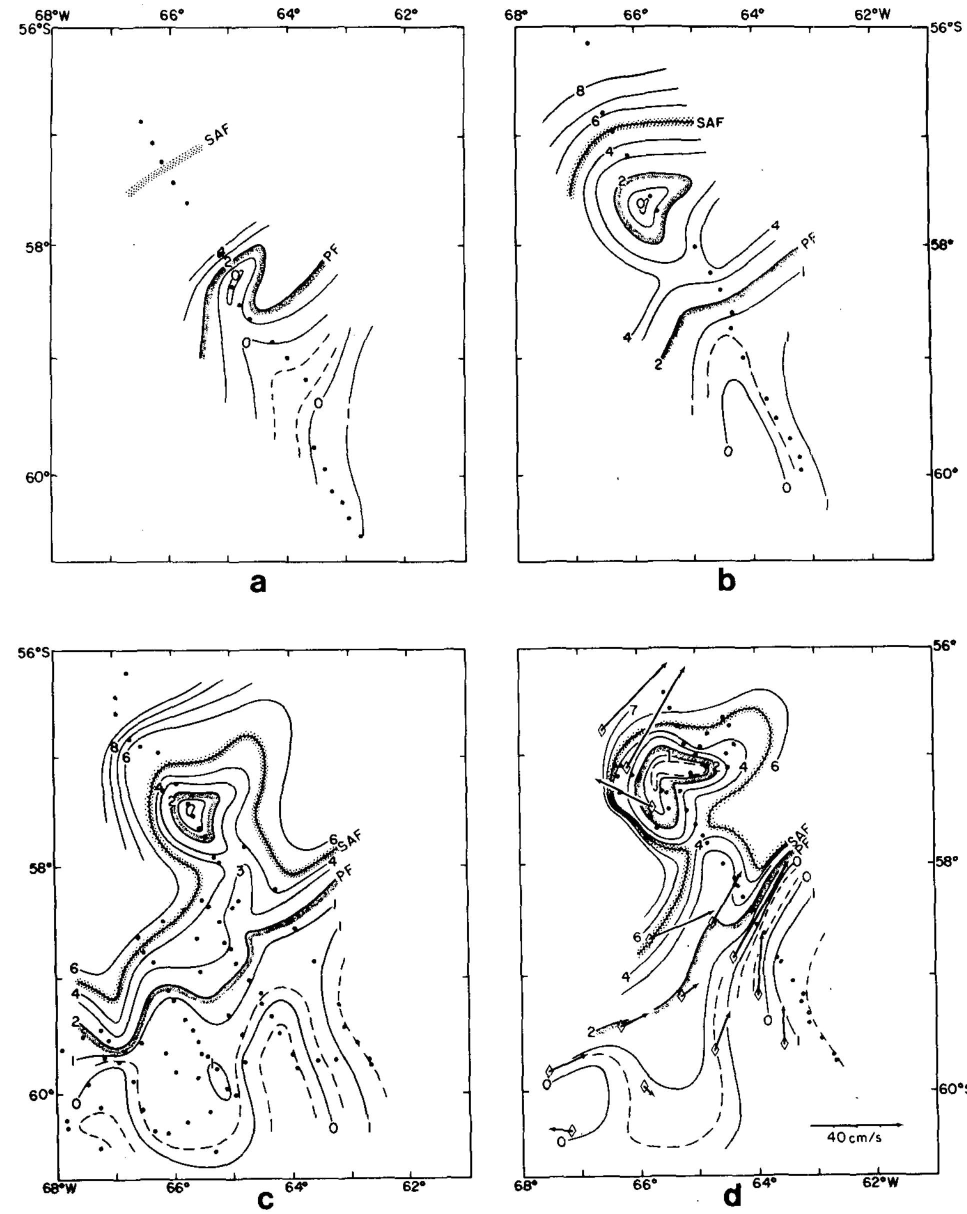

FIG. 4. Distributions of temperature (°C) with frontal positions at 150-m depth during times of *Melville* cruise segments 1 (a), 2 (b), 3 (c) and 4 (d). Included in (d) are 40-h low-pass current vectors from the shallow current meters (500–900 m) during crossing of ring core (4 Feb., 1800 Z).

It was impossible to produce horizontal temperature fields based solely on the first two segments since they were made along straight lines, so the XBT and hydrographic-station temperatures from the second half of the cruise were analyzed first. Since the ring's *T*-minimum was initially located near 150 m, that depth was chosen for the analyses. Data from the fourth segment accurately delineated the ring's thermal geometry, but not that of the adjacent areas. By assuming the patterns to be only slowly changing in time, the fourth-segment geometry was altered slightly to fit the information from the third segment, which provided a description of the areas south and southwest of the ring. Synoptic 40 h low-pass current vectors from the shallow current-meter records (500–900 m) of the moored array were added to the temperature field of the fourth segment. Once the fourth and third segments were analyzed, the patterns were fit to the data from the second, and then the first segment. Fig. 4 shows the resulting time sequence of the ring's thermal evolution at 150-m depth.

Water masses in the ACC can be differentiated by their vertical temperature profiles, as described by Nowlin and Clifford (1982). They found that pro-

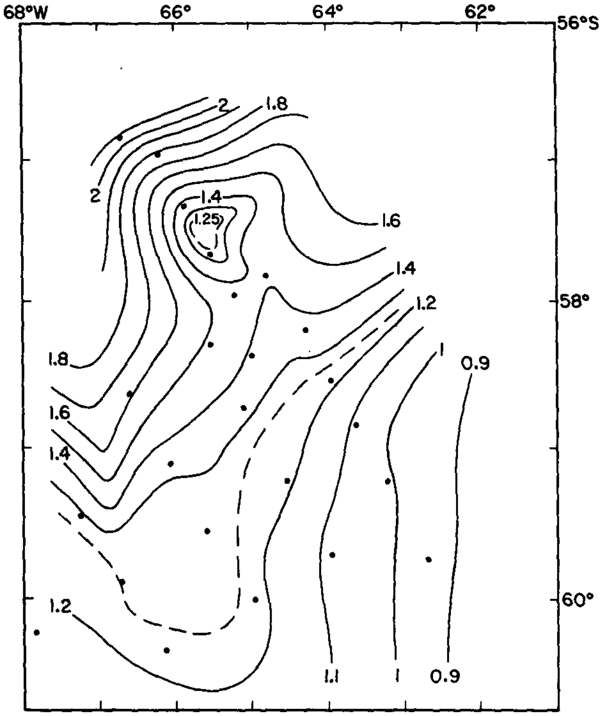

FIG. 5. Geopotential anomaly (dyn. m) of sea surface relative to 2500 m during *Melville* cruise segment 3. The center contour is inferred from extrapolation.

files of T vs Z from hydrographic stations taken from the same side of a specific front consistently fall into the same narrow envelopes from one year to another. By using these envelopes in conjunction with XBT traces, the locations and widths of the fronts can be more accurately determined than by using hydrographic data alone. Using this technique for locating the maximum horizontal density gradients, we found that at 150-m depth the SAF is located near the 5°C isotherm and the PF between the 1.5°C and 2°C isotherms. The CWB remained south of the area of interest. The frontal positions (not necessarily their widths) are indicated in Fig. 4.

The sequence of frontal configurations began with a steep wave (lateral amplitude $\approx$ wavelength) in the PF, which nearly enclosed the northward intrusion of AZ water. Rapid NNW extension of the PF wave at $\sim$14 cm s^{-1} followed. It subsequently pinched off to form an isolated current-ring of cold AZ water within the warmer PFZ while the PF reconnected with itself south of the ring. After the ring separated, it moved NE, slowing to 7 cm s^{-1} as it pushed closer to the SAF. By the end of the cruise, the SAF wave had nearly enclosed the ring, which was $\sim$100 km across and asymmetric.

No hydrographic stations were occupied within the ring during the final segment, when it was nearest to the SAF. But the third-segment survey revealed intense dynamic-topography gradients on the north side of the ring (Fig. 5). Here the surface geostrophic speeds approached 80 cm s^{-1} relative to 2500 m and 90 cm s^{-1} relative to 3500 m. The geostrophic speeds within the individual fronts are normally half these values or less (Nowlin and Clifford, 1982).

During the survey of the central Passage, a shallow layer of warm water poleward of the PF was observed (Fig. 4c). The XBT profiles and hydrographic data showed a vertical transition from southern PFZ characteristics at the surface to AZ features near 100-m depth within this region, which indicates a strong near-surface slant of the PF.

While the disturbance was in its early stages of formation and development, it translated in a direction nearly perpendicular to the mean flow. A detailed bathymetric chart of the study area was constructed and shows that a ridge aligned NW–SE, which rises to nearly 2000 m in places (as compared to surrounding depths of 3500–4500 m), lies downstream of the initial region of cyclogenesis (Fig. 6). The ring's trajectory appears to have followed the ridge toward the NW, and turned NE upon reaching a gap between the ridge and the continental rise. A ring observed in March 1976 formed NE of the ridge in deep water and apparently was not affected by the bathymetry (Joyce and Patterson, 1977).

3. Heat and salt anomalies

Property transports within statically stable water columns by events such as ring formation and move-

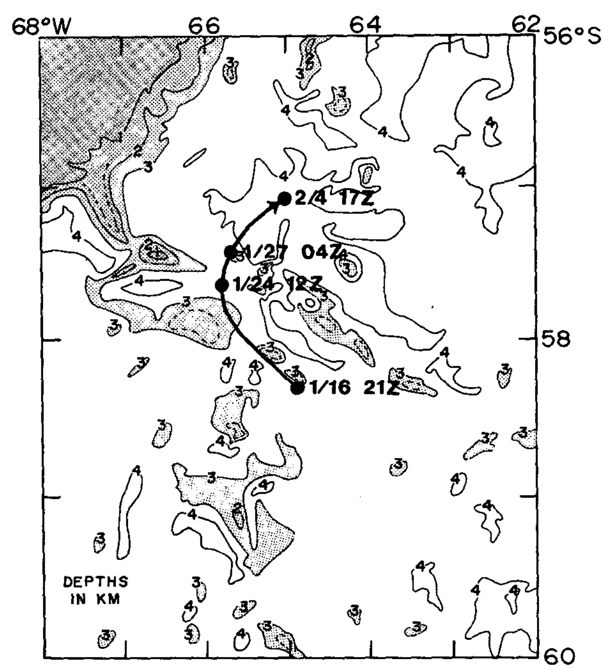

FIG. 6. Bathymetry of central and northern Drake Passage. Path of 1979 cyclonic ring migration and times of core locations indicated.

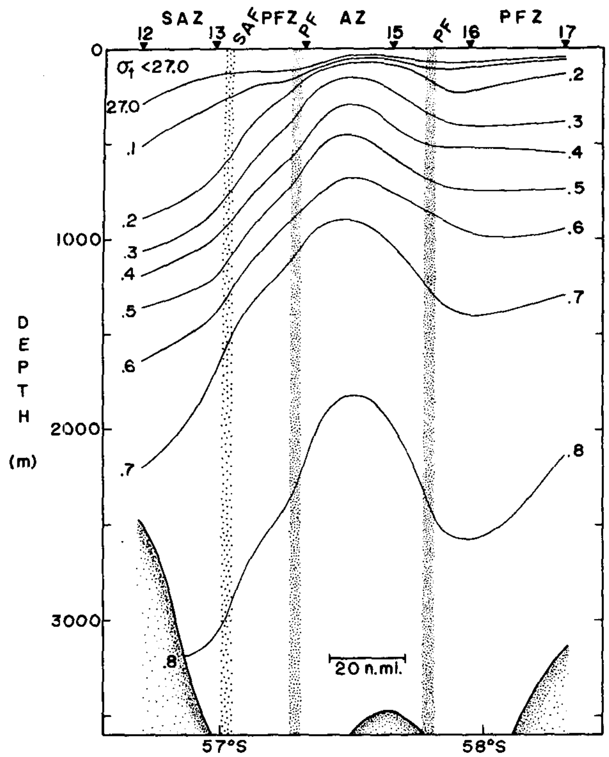

FIG. 7. Distribution of σ_t in vertical section through cyclonic ring from *Melville* cruise segment 3.

ment are best evaluated for layers bounded by isopycnal surfaces. Following the procedure of Joyce *et al.* (1981), the water column between σ_t values of 27.0 and 27.8 was divided into eight layers (Fig. 7). The vertical averages of temperature and salinity for each density layer within the ring are compared with those representative of the same density intervals in water surrounding the ring. The heat anomaly (HA) in Joules per unit horizontal area within a density layer is given as

$$\frac{\text{HA}}{\text{unit area}} = \rho C_p h(\bar{T} - \bar{T}_r),$$

where the density ρ is taken to be constant (1030 kg m^{-3}), C_p is the specific heat capacity at constant pressure (taken to be constant at 4×10^4 J kg^{-1} °C^{-1}), h is the layer thickness within the ring, $\bar{T}$ is the vertically-averaged temperature of that layer at a location within the ring and $\bar{T}_r$ is that for the reference station.

Similarly, the salt anomaly (SA) in kilograms per unit area within a density layer is

$$\frac{\text{SA}}{\text{unit area}} = 0.001\rho h(\bar{S} - \bar{S}_r),$$

where $\bar{S}$ is the vertically-averaged salinity of that layer at a location within the ring and $\bar{S}_r$ is that for the reference station.

Unbiased reference stations are not available from the *Melville* 79 cruise because none of the sections extended through an undisturbed portion of the PFZ or SAZ (i.e., where there were no significant effects of the ring or warm lens). Since the characteristics of the water types on the same side of a specific front remain uniform through time (Nowlin and Clifford, 1982), reference stations from a cruise which typifies the mean may be used. The vertically-averaged tem-

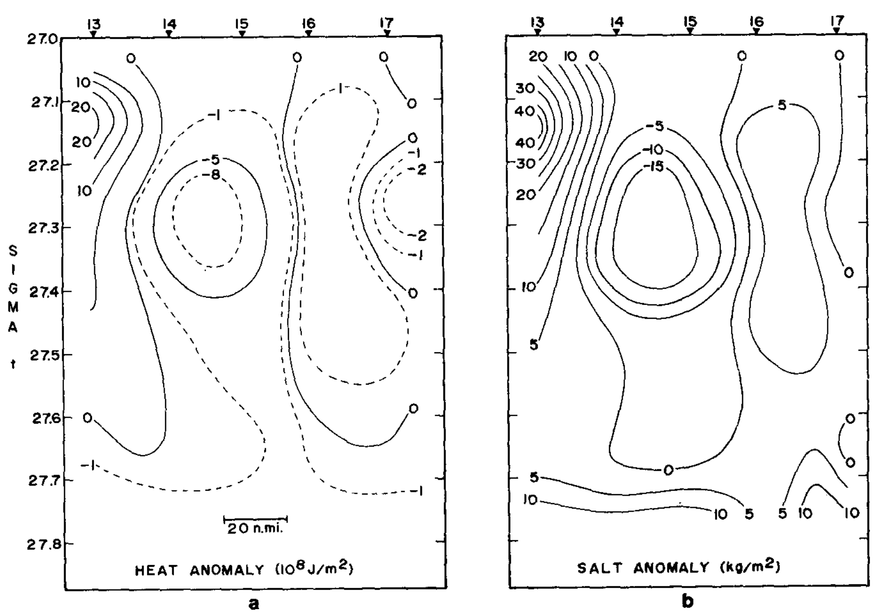

FIG. 8. (a) Heat anomaly and (b) salt anomaly in vertical section through cyclonic ring from *Melville* cruise segment 3. Averaged distributions of temperature and salinity observed in PFZ on *Thompson* 1976 cruise used as references.

peratures and salinities within each density layer from the *Thompson* 76 transect in Fig. 1 were horizontally-averaged across the PFZ and SAZ, and are used as our reference stations.

Our estimations of HA and SA were first made by using the PFZ as a reference (Fig. 8). The anomalies are treated as being linear functions of radial distance between isopleths in a ring-centered coordinate system. For example, the heat anomaly of the layer extending from σ_{t_1} to σ_{t_2} is

$$\mathrm{HA}\Big|_{\sigma_{t_2}}^{\sigma_{t_1}} = \int_0^{2\pi}\int_0^R [\mathrm{HA}(r)]rdrd\theta,$$

where R is the average radius for which HA(r) is zero.

Since a clear ring signature only extended down to $\sigma_t = 27.7$ in the anomaly fields, even though the density perturbations appeared throughout the water column (Fig. 7), evaluation of the total anomalies was terminated there. The total heat and salt anomalies for this ring and for the March 1976 ring (Joyce *et al.*, 1981) with respect to the PFZ are given in Table 1. Our values are about two-thirds of those obtained by Joyce *et al.* for the earlier ring. The discrepancies may be accounted for by differences in ring sizes and in reference station properties. But, the comparisons are favorable and indicate a consistency in the magnitude of the heat and salt transports effected by Drake Passage rings. Gordon (de Szoeke and Levine, 1981) has estimated the poleward heat flux required to balance the air–sea heat loss around Antarctica to be 3×10^{14} W and Gordon and Taylor (1975) estimated the poleward salt flux needed to balance the precipitation surplus as 10^7 kg s^{-1}. The formation of three to four rings of this size per day from PF meanders along the ACC would satisfy these requirements. But other transfer processes, such as the cross-isotherm flow in baroclinic waves, the northward movement of Antarctic Bottom Water, and interleaving within the PF (Joyce *et al.*, 1978), are also important in the heat and salt budgets of the Southern Ocean.

By the end of the cruise, the ring appeared to be on the verge of breaking through the SAF. On the chance that this event may have occurred, a comparison was made between the ring and the SAZ reference station. The total anomalies for this reference are also given in Table 1. These are about four times larger than those referred to the PFZ, which would satisfy a one-day requirement of the heat and salt budgets of the Southern Ocean.

TABLE 1. Total heat and salt anomalies for cyclonic rings observed at Drake Passage.

	1976 Ring, Joyce *et al.* (1981), referred to PFZ	1979 Ring, referred to PFZ	1979 Ring, referred to SAZ
Heat	-1.2×10^{19} J	-8×10^{18} J	-3×10^{19} J
Salt	-2.5×10^{11} kg	-2×10^{11} kg	-8×10^{11} kg

4. Hydrodynamic stability of zonal flow

Here we consider the necessary conditions for baroclinic and barotropic instabilities based on the linearized perturbation theory introduced by Charney (1947) and Eady (1949). Our initial, basic-state flow regime is that from the same *Thompson* 76 transect used before. It would be inappropriate to use a mean flow regime, because once the properties of instantaneous states are averaged and smoothed, a more stable situation may result than would actually exist in a real initial state. In this transect, the fronts occupied positions close to their means and the frontal widths and core speeds were within their typical ranges, making this a suitable flow regime to use as a basic state.

The meridional gradient of potential vorticity, Q_y, is given by

$$Q_y = \beta - U_{yy} - f^2\left(\frac{U_z}{N^2}\right)_z,$$

where β is the latitudinal variation of the Coriolis parameter, U is the zonal current speed, f is the local Coriolis parameter and N is the Brunt-Väisälä frequency.

For the purely barotropic case, vertical variations of geostrophic velocities were eliminated by taking vertical averages. After fitting a smooth curve to the vertically-averaged velocity field, the U_{yy} field was evaluated. A necessary condition for barotropic instability is that $\beta - U_{yy}$ be negative. In Fig. 1, the double contours demark regions where horizontal shears may produce barotropic instability.

For the purely baroclinic case, lateral variations in velocity were ignored while the vertical structure was examined. The necessary condition for baroclinic instability can be satisfied, among other ways, if Q_y changes sign within the water column. Evaluation of Q_y was performed for each station pair comprising the basic state. The averaged N^2 profiles for each zone from the 1975 and 1976 ISOS cruises were used (Fig. 9a). The N^2 profiles from the zones bordering the individual fronts were averaged to characterize stations within a front. For the basic state, each Q_y profile changed sign two or more times within the water column, thus satisfying the necessary condition for baroclinic instability. Figs. 9b and 9c show the U_z and Q_y profiles of three station pairs that extend from one side of the PF to the other. The necessary condition was met even in the regions of weak vertical shear, so the entire zonally-oriented basic flow regime may have been baroclinically unstable. To be certain of this would require the calculation of growth rates, which is not done here.

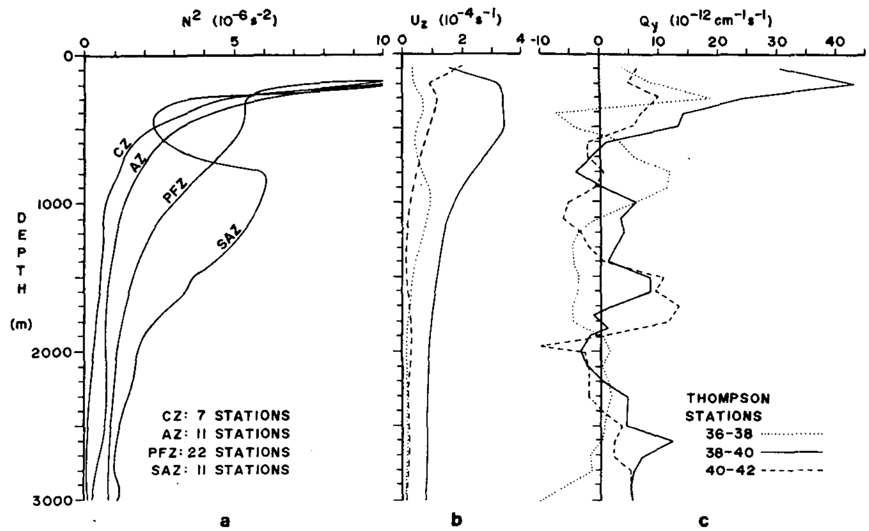

FIG. 9. (a) Vertical profiles of N^2 for water-mass zones at Drake Passage obtained by averaging data from 1975 and 1976 ISOS cruises. Vertical profiles of U_z (b) and Q_y (c) for indicated *Thompson* 1976 station pairs. See Fig. 1 for locations.

5. Discussion

The zonal flow of the basic state showed the potential for baroclinic instability everywhere and for barotropic instability adjacent to the three fronts. An equatorward perturbaton on the PF may grow, and in doing so, would disturb the flow farther north. Cross-stream displacement of such a disturbance might result. This appears to have happened during the DRAKE 79 cruise of the *Melville*. These observations show that a cold-core cyclonic ring formed from a PF meander and progressed across the PFZ toward the SAF. The combined horizontal density gradients of the ring and those of the SAF produced surface geostrophic speeds of up to 90 cm s^{-1} relative to 3500 m. These large speeds, which are double the usual core speeds in ACC fronts, probably result frequently as rings impinge on fronts within the system. The resulting vertical and horizontal shears may then produce a more unstable situation than in the basic state.

There is no evidence concerning the ultimate fate of ACC rings, but our observations and stability analysis indicate that this one may have entered the SAZ. The deepening of the *T*-minimum layer of the ring core during its northward movement corresponds to the slight inclination of isopycnal surfaces within the PFZ of the basic state (Fig. 10). During the deepening, the surface temperature contrast across the ring had diminished from 3–4°C initially

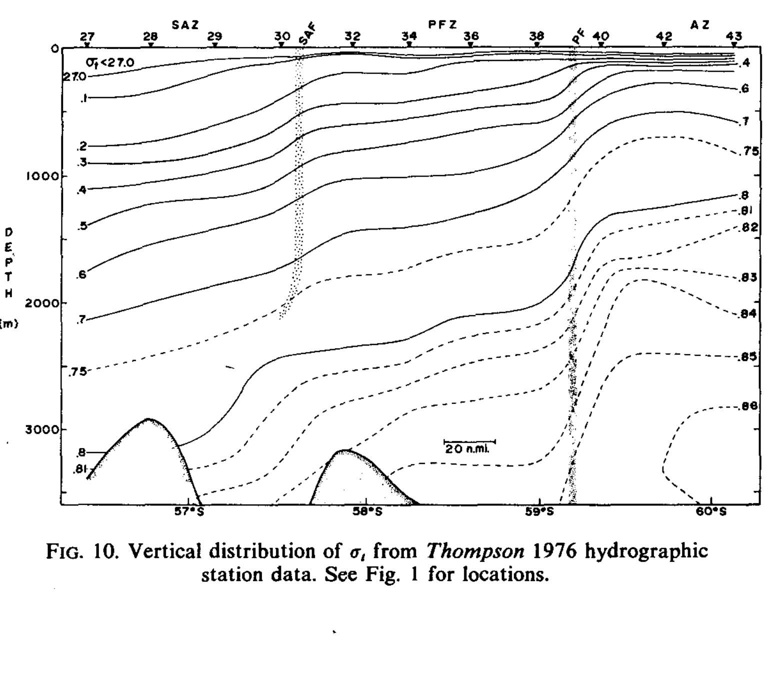

FIG. 10. Vertical distribution of σ_t from *Thompson* 1976 hydrographic station data. See Fig. 1 for locations.

to less than 2°C by the time of our final observations. If the ring crossed the SAF, continued deepening of the *T*-minimum layer and surface mixing may have reduced the surface thermal expression to the extent that it became undetectable by satellite IR imagery. Should this be the general case, an estimate of the Southern Ocean ring inventory cannot be made by currently available remote sensing techniques.

Most of the anomalies associated with the ring core were found from σ_t = 27.2 to 27.4. The mid-depth of this layer deepened rapidly, to about 1000 m, north of the SAF in both this study and the *Thompson* 76 transect (Figs. 7 and 10). Most of the ring's influence would have been realized within that layer, which is where the Antarctic Intermediate Water (AAIW) is found farther north. The processes by which AAIW is formed are not clearly understood. The Subantarctic Mode Waters, which are presumed to be formed by air–sea interactions within the SAZ at selected locations, are thought to be a source water for AAIW (McCartney, 1977), as are the waters of the AZ and southern PFZ (Molinelli, 1978). The average temperature and salinity values for AAIW entering the Atlantic within the σ_t = 27.2 to 27.3 layer are 2.9°C and 34.18 per mille (Molinelli, 1981). Provided that the SAF wave pinched off, about 1.7×10^{12} m^3 of AZ and PFZ water, with volume-averaged values of 2.5°C and 34.13‰, would have been transported into the SAZ within that layer. This water would become warmer and more saline after mixing with SAZ water. Should ring movement into the SAZ prove to be a recurrent event, rather than an isolated or hypothetical one, the water-mass exchanges involved may represent one of the sources for AAIW as well as an enhanced contribution by rings to the heat and salt budgets of the Southern Ocean.

Acknowledgments. This work was sponsored as part of the International Southern Ocean Studies by the National Science Foundation, Office for the International Decade of Ocean Exploration. We would like to thank Masamichi Inoue for his calculations of the averaged N^2 profiles for each zone.

REFERENCES

Bryden, H. L., 1979: Poleward heat flux and conversion of available potential energy in Drake Passage. *J. Mar. Res.*, **37**, 1–22.

——, 1981: The Southern Ocean. *Eddies in the Ocean*, A. R. Robinson, Ed., SCOR, Chap. 14 (in press).

Charney, J. G., 1947: The dynamics of long waves in a baroclinic westerly current. *J. Meteor.*, **4**, 135–163.

Deacon, G. E. R., 1937: The hydrology of the Southern Ocean. *Discovery Rep.*, **15**, 1–124.

deSzoeke, R. A., and M. D. Levine, 1981: The advective flux of heat by mean geostrophic motions in the Southern Ocean. *Deep-Sea Res.*, **28A**, 1057–1085.

Eady, E. I., 1949: Long waves and cyclone waves. *Tellus*, **1**, 33–52.

Gordon, A. L., H. W. Taylor and D. T. Georgi, 1974: Antarctic oceanographic zonation. *Proc. SCOR/SCAR Polar Oceans Conference*, Montreal, I.O.C., 682 pp.

——, and ——, 1975: Heat and salt balance within the cold waters of the world ocean. *Numerical Modes of Ocean Circulation*, Nat. Acad. Sci., pp. 54–56.

——, D. T. Georgi and H. W. Taylor, 1977: Antarctic Polar Front zone in the western Scotia Sea—summer 1975. *J. Phys. Oceanogr.*, **7**, 309–328.

Joyce, T. M., and S. L. Patterson, 1977: Cyclonic ring formation at the Polar Front in the Drake Passage. *Nature*, **265**, 131–133.

——, W. Zenk and J. M. Toole, 1978: The anatomy of the Antarctic Polar Front in the Drake Passage. *J. Geophys. Res.*, **82**, 6093–6113.

——, S. L. Patterson and R. C. Millard, Jr., 1981: Anatomy of a cyclonic ring in the Drake Passage. *Deep-Sea Res.*, **28A**, 1265–1287.

Mackintosh, N. A., 1946: The Antarctic convergence and the distribution of surface temperature in Antarctic Waters. *Discovery Rep.*, **23**, 177–212.

McCartney, M. S., 1977: Subantarctic Mode Water. A Voyage of Discovery, M. Angel, Ed. *Deep-Sea Res.*, **24**(suppl.), 103–119.

Meinardus, W., 1923: *Meteorologische Ergebnisse der Deutsche Südpolar-Expedition, 1901–1903.* Deutsche Südpolar-Expedition. III. Meteorologie, Bd. 1, Heft 1.

Molinelli, E. J., 1978: Isohaline thermoclines in the southeast Pacific Ocean. *J. Phys. Oceanogr.*, **8**, 1139–1145.

——, 1981: The Antarctic influence on Antarctic Intermediate Water. *J. Mar. Res.*, **39**, 267–293.

Nowlin, W. D., Jr., T. Whitworth and R. D. Pillsbury, 1977: Structure and transport of the Antarctic Circumpolar Current at Drake Passage and short-term measurements. *J. Phys. Oceanogr.*, **7**, 788–802.

——, and M. A. Clifford, 1982: The kinematic and thermohaline zonation of the ACC at Drake Passage. *J. Mar. Res.* (in press).

Savchenko, V. G., W. J. Emery and D. A. Vladimirov, 1978: A cyclonic eddy in the Antarctic Circumpolar Current south of Australia: Results of Soviet–American observations aboard the R/V *Professor Zubov*. *J. Phys. Oceanogr.*, **8**, 825–837.

Whitworth III, T., 1980: Zonation and geostrophic flow of the Antarctic Circumpolar Current at Drake Passage. *Deep-Sea Res.*, **27**, 497–507.

Wright, D. G., 1981: Baroclinic instability in Drake Passage. *J. Phys. Oceanogr.*, **11**, 231–246.